RSC Advances

PAPER

View Article Online
View Journal | View Issue

Cite this: *RSC Adv.*, 2014, **4**, 43098

One step synthesis of maltose functionalized red fluorescent Ag cluster for specific glycoprotein detection and cellular imaging probe†

SK Basiruddin*[ab] and Atanu Chakraborty[b]

Received 6th July 2014
Accepted 27th August 2014

DOI: 10.1039/c4ra06723a

www.rsc.org/advances

The synthesis of non-cadmium based carbohydrate functionalized inorganic fluorescent nanoparticles has emerging potential applications in advanced biomedical science. Herein, we synthesized red fluorescent maltose functionalized silver clusters (AgC) using cysteamine modified maltose as a capping agent without adding any external reductant. The silver clusters had a hydrodynamic diameter of less than 5 nm with good colloidal, photochemical and fluorescent stability with a reasonably good fluorescence quantum yield. Maltose functionalized fluorescent silver clusters were produced in a one step procedure. Therefore, we exploited the maltose functionalized silver clusters for the visible detection of specific glycoprotein concanavalin-A. Because the synthesized red fluorescent maltose functionalized silver clusters possesses good photochemical stability and green light excitation, we used maltose functionalized red fluorescent AgC for HeLa cell labelling study.

Introduction

Fluorescent noble metal nanoclusters are very important for biological applications. Conventional organic dyes are photo-chemically unstable and significantly small to be used as fluorescent probes. Highly fluorescent photo-chemically stable cadmium based quantum dots are tremendously toxic for biomedical applications[1,2] and require surface engineering as well as proper functionalization for biological applications.[3–10] The synthesis of fluorescent probes with a reasonable size, non-toxicity along with well decorated targeted biomolecule functionalization is exciting the scientific community, who are working in the field of cellular and sub cellular targeting as well as *in vivo* targeting of nanoparticle based drug delivery.[11–15] In this regard, noble metal nanoclusters are potential nano-materials. Noble nanoclusters with a size (<2 nm) comparable to the Fermi wavelength of an electron exhibit some exciting properties that are not shown by their nanoparticle counterparts.[16] Fluorescent Ag clusters are attracting the scientific community because of their visible excitation, near-IR emission, excellent photo-stability, small size, reasonable quantum yield, and lower toxicity than quantum dots (QDs). The synthesis of Ag clusters involves the reduction of Ag^{1+} to Ag^{0} in the presence of a suitable capping agent by microwave assisted,[17] photo chemical,[18] sonochemical,[19,20] chemical and other methods.[21–25] Various stabilizing ligands like proteins,[26] peptides,[27] DNA,[28–31] aptamers,[24,32] polymers,[33] and many other small ligands have been exploited to synthesize fluorescent silver clusters (AgC). However, carbohydrate or sugar stabilized fluorescent AgC has not been reported to the best of our knowledge. Here, we synthesized carbohydrate functionalized red fluorescent AgC.

Carbohydrates are the most important biomolecules in living systems. Cell membranes are coated with a dense coating of carbohydrate based macromolecules like glycoproteins and glycolipids. In glycoproteins/lipids, carbohydrates remain conjugated with proteins and lipids. Some carbohydrate receptors are over expressed in many cancer cell lines. An over expressed carbohydrate receptor can be used to detect, image and diagnose cancer in the early stages, or numerous other diseases. Carbohydrate functionalized nanoparticles are used in protein detection, pathogen detection, in the study of carbohydrate–protein interaction, organ specific distribution in mouse model, selective cancer targeting and therapy, and many other potential biological applications.[34–38] Therefore, the synthesis of carbohydrate functionalized fluorescent AgC is significantly important for advanced applications in the field of biomedical science.

Here, we prepared maltose functionalized red fluorescent AgC using cysteamine modified maltose as a capping agent. Maltose is a disaccharide formed from two units of glucose joined with an $\alpha(1 \rightarrow 4)$ bond. Maltose has a reducing end (formyl group) group, which can be chemically linked to NH_2 group of cysteamine through reductive amination and it can be

[a]*Veer Surendra Sai University of Technology, Department of Chemistry, Burla, Sambalpur-768018, India. E-mail: sk.basi@gmail.com*

[b]*Indian Association for the Cultivation of Science, Jadavpur, Kolkata, 700032, India*

† Electronic supplementary information (ESI) available: Supporting data like HR-Mass, NMR, FT-IR, XPS, TEM, EDS, MALDI-TOF mass, DLS, Zeta potential measurement, MTT assay, cell images and other important data are available in ESI. See DOI: 10.1039/c4ra06723a

used as a stabilizing agent in the preparation of red fluorescent AgC. Therefore, maltose functionalized red fluorescent AgC has glucose molecules exposed on their surface. We used maltose (or glucose) functionalized red fluorescent Ag clusters for the spectroscopic detection of specific glycoprotein as well as by the naked eye. Moreover, maltose functionalized red fluorescent Ag clusters are photochemically stable with low photo bleaching property and have excitation in visible light ($\lambda_{max} \sim 510$ nm). We applied maltose functionalized red fluorescent AgC as a cellular imaging probe for HeLa cancer cells.

Experimental section

Materials

Maltose monohydrate, cysteamine hydrochloride, sodium cyanoborohydride [$Na(CN)BH_3$], sodium borohydride ($NaBH_4$), $AgNO_3$, oleylamine, oleic acid, D_2O, concanavalin-A (Con-A), bovine serum albumin (BSA), microcentrifuge filters (0.45 μm), and dialysis membrane (MWCO 12–14 kDa) were purchased from Sigma Aldrich and used as received.

Preparation of cysteamine modified maltose (maltose-SH) by reductive amination

Cysteamine functionalized maltose was prepared by a sodium cyanoborohydride ($Na(CN)BH_3$) based reductive amination method. Typically, 360 mg (1 mmol) maltose monohydrate and 113.6 mg (1 mmol) cysteamine hydrochloride were dissolved in 4 mL of water. Then, 400 μL of 0.1 M borate buffer of pH 9 was added to the reaction mixture. Subsequently, 2 mmol of $Na(CN)BH_3$ was added and the reaction mixture was stirred for 72 hours. After the completion of the reaction, 10 folds amount of ethanol with respect to the reaction mixture was added to precipitate the cysteamine modified maltose (maltose-SH) from the solution, leaving the unreacted cysteamine in solution. The precipitate was collected and dissolved in a minimum amount of fresh water. Again, ethanol was added to precipitate the maltose-SH from the solution. This precipitation–redispersion method was repeated for more than three times to make the cysteamine free from maltose-SH.

Synthesis of maltose functionalized red fluorescent Ag cluster (AgC)

First, hydrophobic silver-oleylamine/oleic acid complex was synthesized by dissolving 17 mg of $AgNO_3$ with 200 μL of oleylamine and 200 μL of oleic acid in 4 mL toluene. Then, 80.6 mg of maltose-SH (dissolved in 4 mL DMSO with a small amount (100 μL) of water) was added to the silver–oleylamine complex and vigorously shaken for 60 minutes. Subsequently, the solution was allowed to settle. Two distinct layers of toluene and DMSO were formed. The DMSO layer containing red fluorescent AgC was separated by a micro pipette. Then, an equal volume of absolute alcohol was added to the DMSO solution of maltose functionalized AgC. The maltose functionalized AgC was precipitated and collected by centrifuging at 5000 rpm for 5 minutes; it was then dissolved in double distilled water and stored at 4–8 °C until further use.

Quantum yield (QY) measurement

The QY of the maltose functionalized red fluorescent AgC was measured using rhodamine B as the reference (QY = 31% at 510 nm excitation). The formula used for the QY measurement is as follows:

$$(QY)_{Sm} = (QY)_{St} \frac{(PL_{area}/OD)_{Sm}}{(PL_{area}/OD)_{St}} \frac{\eta_{Sm}{}^2}{\eta_{St}{}^2}$$

where Sm indicates the sample, St indicates the standard, η is the refractive index of the solvent, "PL area" indicates the fluorescence area, and OD indicates the absorbance value.

Specific glycoprotein detection by maltose functionalized red fluorescent AgC

We performed a specific glycoprotein detection study using maltose functionalized red fluorescent AgC. For the investigation, two sets of photoluminescence (PL) cuvettes, each containing 2 mL of maltose functionalized red fluorescent AgC solution of pH 7.4, were taken. Subsequently, 200 μL of 100 μM of Con-A was added to one of the cuvettes. Whereas 200 μL of 100 μM of BSA was added to another cuvette, which was used for the control experiment. Selective binding between the Con-A and maltose functionalized red fluorescent AgC leads to particle aggregation (Fig. 5A), which was observed within few minutes after mixing of Con-A. However, no precipitation was observed when BSA was added to the maltose functionalized red fluorescent AgC solution (Fig. 5B).

Cellular labelling and imaging

Human cervical cancer HeLa cells were cultured in Dulbecco's modified eagle medium (DMEM) supplemented with 10% fetal bovine serum (FBS) and 1% penicillin/streptomycin at 37 °C and under an atmosphere of 5% CO_2. For cellular labelling studies, HeLa cells were seeded into 4-well chamber slides. After the overnight growth of HeLa cells on the chamber slides, red fluorescent maltose functionalized AgC were added to reach final concentrations of 0.2–1.0 mg mL^{-1}, and incubated for 2 h. Subsequently, the cells were washed with copious amount of PBS buffer solution to remove the unbound red fluorescent maltose functionalized AgC, and then fixed with 4% paraformaldehyde, mounted with 50% glycerol and used for the microscopic cellular imaging study.

Cell viability study of maltose functionalized red fluorescent AgC by MTT assay

The relative cytotoxic effect of the maltose functionalized red fluorescent AgC was evaluated using the conventional 3-(4,5-dimethylthiazol-2-yl)-2,5-diphenyltetrazolium bromide (MTT) based colorimetric assays. The HeLa cells were seeded into 24-well plates at high density in the DMEM media supplemented with 10% FBS and 1% penicillin/streptomycin at 37 °C and under an atmosphere of 5% CO_2. After overnight growth, the cells were incubated with the maltose functionalized red fluorescent AgC of different final concentrations (0.1–0.5 mg mL^{-1}) for 24 h. Next, the cells were washed with PBS buffer solution,

followed by the addition of 500 μL of fresh DMEM into each well. Then, 50 μL of an aqueous solution of MTT (5 mg mL^{-1}) was added into each well and incubated for 4 h. Violet formazan was dissolved in sodium dodecyl sulphate (SDS) solution prepared in a water–DMF mixture, and the absorbance was measured at 570 nm using a microplate reader. The relative cell viability was measured assuming 100% cell viability for the control cells without any maltose functionalized AgC.

Instrumentation

The UV-Vis absorption spectra were recorded on a Shimadzu UV-2550 UV-Vis spectrophotometer, and the fluorescence measurements were performed on a BioTek Synergy Mx microplate reader. Transmission electron microscopy (TEM) images were obtained using a JEOL-JEM 2010 electron microscope. The 1H (500 MHz) spectra were recorded on a Bruker DPX-500 spectrometer at room temperature. Fourier transform infrared (FTIR) spectra of KBr powder-pressed pellets were recorded on a Perkin-Elmer Spectrum 100 FTIR spectrometer. X-ray photoelectron spectroscopy (XPS) was performed using an Omicron (serial no. 0571) X-ray photoelectron spectrometer. Time correlated single photon counting (TCSPC) was performed by exciting the sample with a picoseconds diode laser (IBH Nanoled) using a Horiba Jobin Yvon IBH Fluorocube apparatus. Dynamic light scattering (DLS) and zeta potential were measured using a NanoZS (Malvern) instrument. MALDI-TOF spectra of the red fluorescent AgC was measured with a MALDI TOF Ultraflextreme (Bruker Daltonics) instrument using 2,5-dihydroxybenzoic acid (DHB) as the matrix. Fluorescence imaging and the photo-stability of nanoparticles were performed by drop casting the sample solution on a glass slide and the cell images were taken under the filter set up (excitation – 480–550 nm and emission collected after 590 nm) of an Olympus IX81 microscope using a camera Photometrics Cool-Snap Cf2, with an exposure time of 2 seconds. The bright and fluorescent images of the cells were obtained using an Olympus IX81 microscope using image-pro plus version 7.0 software.

Results and discussion

Maltose functionalized red fluorescent AgC were prepared from Ag-oleylamine/oleic acid complex using a stabilizing agent cysteamine modified maltose (maltose-SH) in the toluene/DMSO bilayer (Scheme 1/C). First, cysteamine modified maltose was synthesized using a sodium cyanoborohydride based reductive amination method between cysteamine and maltose.[39] Maltose has a reducing carbonyl (C=O) end group in an open chain form or in a cyclic pyranose form. The carbonyl group reacts with an amine group to form imine bond, which is reduced to form cysteamine modified maltose (maltose-SH) in the presence of sodium cyanoborohydride (Scheme 1/A). The successful preparation of cysteamine modified maltose was characterized by HR Mass, FT-IR, XPS and NMR spectroscopy. In the HR-Mass spectrum (ESI, Fig. S1 & S2†), the peak at 365.0742 was assigned to maltose (*i.e.*, maltose + Na), whereas the peak at 429.0250 was assigned to cysteamine modified maltose (*i.e.*, maltose-SH + Na^+ + $3H^+$). In the FTIR spectrum (ESI, Fig. S4†), peak at 1650 cm^{-1} was attributed to the bending

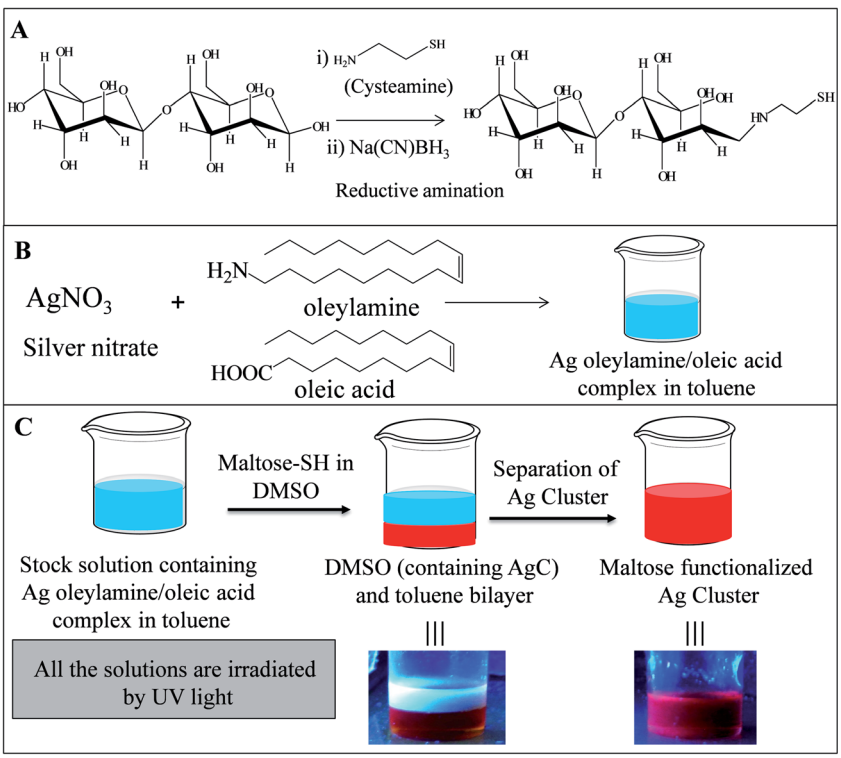

Scheme 1 Synthesis of maltose functionalized red fluorescent silver clusters (AgC).

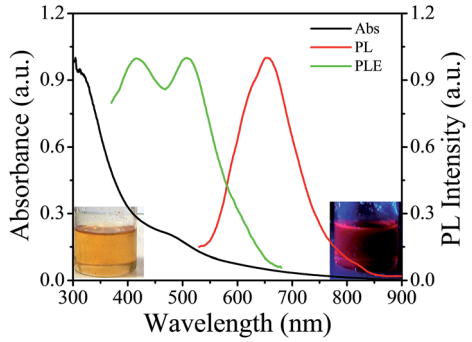

Fig. 1 Optical properties of red fluorescent silver clusters (AgC). Typical absorption (black line), excitation (green line) and photoluminescence (red line) spectra of maltose functionalized red fluorescent AgC in water. Insets show digital images of AgC in normal light (left side) and under UV light (right side).

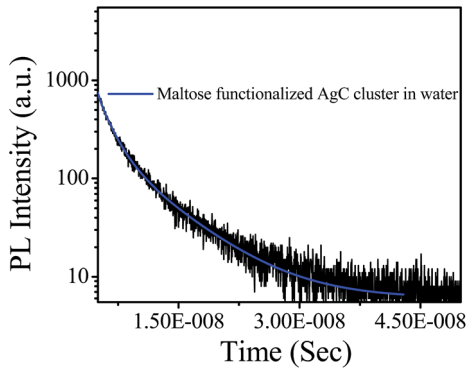

Fig. 2 Fluorescence lifetime of red fluorescent AgC in water with excitation at 440 nm and detection at 655 nm (red).

vibration of the secondary amine of maltose-SH, which is also supported by the peaks at 401.5 eV in the XPS spectrum of the N1s binding energy of the secondary amine (ESI, Fig. S6†). In 1H-NMR spectroscopy, the δ value of protons between 3.25 to 4 ppm was assigned to the maltose carbohydrate moiety and the absence of peak at δ value of 5.3 ppm was attributed to the protons at the reducing end of maltose in maltose-SH (ESI, Fig. S3†). The reducing end H atom disappeared because of the conjugation between cysteamine and maltose. The results indicate the successful synthesis of maltose-SH from cysteamine and maltose by reductive amination.

We synthesized red fluorescent AgC using a bilayer approach. A bilayer formed by an equal volume of toluene, containing Ag-oleylamine/oleic acid complex, and DMSO, containing cysteamine modified maltose (maltose-SH) and small amount of water as an impurity. Without the addition of water, toluene and DMSO cannot form a bilayer as they are miscible. After making of the aforementioned bilayer, the mixture was vigorously vortexed for 30 minutes. During vortex mixing, maltose-SH reacts with the Ag-complex to form a maltose-SH capped yellow colored AgC solution in the DMSO layer. This yellow colored solution emits red fluorescence under UV light excitation. Red fluorescent AgC were separated from the DMSO solution by precipitating the Ag clusters by adding a certain amount of absolute alcohol; maltose is insoluble in absolute alcohol. Because the AgC is capped by the cysteamine functionalized maltose, therefore the addition of a certain amount of alcohol results in the precipitation of AgC from the DMSO solution. Precipitate of red fluorescent AgC was then dissolved in distilled water.

XPS data shows that the AgC are mainly composed of Ag^{1+}, which is also supported by the $NaBH_4$ test (ESI, Fig. S10†). Addition of certain amount of $NaBH_4$ to the Ag cluster caused the reduction of Ag^{1+} to Ag^0 and an increase in the cluster size (Fig. S10(A)†). The oxidation state of Ag in maltose functionalized red fluorescent AgC was verified by XPS. Fig. 4 shows the XPS spectrum in the Ag 3d region. The observed peaks of Ag $3d_{5/2}$ and Ag $3d_{3/2}$, at 370 and 376 eV, respectively, confirm the existence of silver in the Ag^{1+} form.[40] The size of the maltose functionalized AgC was investigated by transmission electron microscopy (TEM) and dynamic light scattering (DLS). TEM data shows only a core nanoparticle of ~1.8 nm in diameter, where the thin cysteamine modified maltose shell is invisible due to their low electron density (Fig. 3). However, DLS study shows an overall diameter of inorganic core silver cluster as well as hydrated cysteamine modified maltose, which ranges from 2–6 nm (ESI, Fig. S11†). The optical property of the maltose functionalized AgC was characterized by UV-Visible, photoluminescence (PL) spectroscopy and time correlated single photon counting (TCSPC) measurement system. Maltose functionalized AgC shows a broad peak centered at 480 nm in the UV-Visible absorption spectrum, and two maxima at 410 nm and 510 nm in the photoluminescence excitation (PLE) spectrum. Both excitation maxima gave the same photoluminescence spectra centered at 655 nm (Fig. 1). It did not show any excitation dependent fluorescence property. The fluorescence quantum yield of the maltose functionalized red fluorescent AgC was found to be 3% in water, taking rhodamine-B as the reference. The exponential decay curve of time correlated single photon counting (TCSPC) measurements fitted the life time values ($T_1 = 0.132$ ns, $T_2 = 0.72$ ns, $T_3 = 2.42$ ns and $T_4 = 7.1$ ns) and their relative contributions ($B_1 = 11.02$, $B_2 = 24.11$, $B_3 = 36.22$ and $B_4 = 28.65$), which indicates the heterogeneous size distribution of maltose functionalized AgC

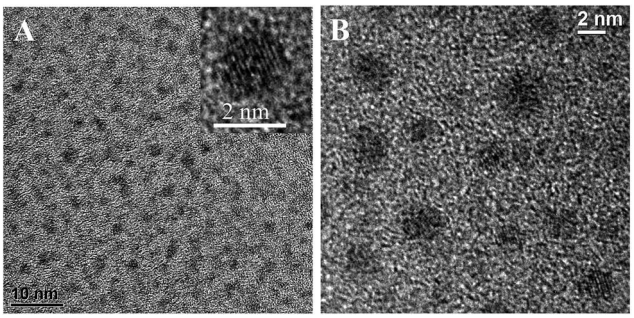

Fig. 3 TEM image of silver clusters (AgC) at different scales (A & B). The samples were dropcasted on a carbon-coated copper grid and images are taken by TEM. Inset shows an HRTEM image of the red fluorescent AgC of size ~1.8 nm (left panel).

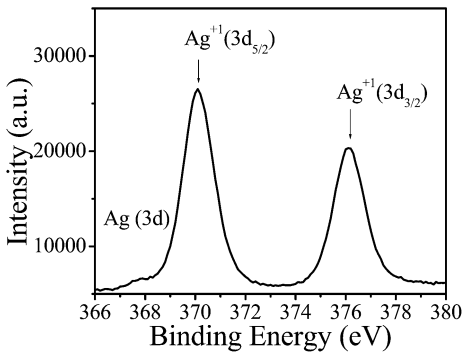

Fig. 4 XPS data of Ag cluster (AgC). XPS spectrum is in the Ag 3d region of Ag. The characteristics peaks of Ag $3d_{5/2}$ at 370 eV and that of Ag $3d_{3/2}$ at 376 eV indicate the existence of silver in its Ag^{1+} state in the red fluorescent AgC.

(Fig. 2), which is approximately 2 nm. Therefore, the average PL lifetime of these AgC was found to be 3 ns.

Maltose functionalized red fluorescent AgC has great potential for biomedical applications. The silver cluster is stabilized by bio-friendly and biocompatible carbohydrate molecule maltose, which has a glucose end group. Thus, maltose functionalized AgC has been used for the detection of specific glycoprotein conconavalin-A (Con-A). Conconavalin-A is a glycoprotein with four binding sites for a glucose molecule at pH 7.4. One Con-A protein simultaneously binds with four glucose molecules. Moreover, maltose functionalized red fluorescent AgC have glucose molecules on their surface. On addition of Con-A to the maltose functionalized AgC solution, Con-A simultaneously binds with the glucose molecule of different AgC. Therefore, Con-A crosslinks the silver clusters. As a result, AgC gets precipitated from the solution and its characteristic fluorescence intensity in the supernatant solution gets decreased. In addition, bovine serum albumin (BSA) was taken as a control experiment to determine the specificity of binding affinity between the Con-A and maltose functionalized AgC. If maltose functionalized AgC does not have binding specificity to Con-A, then the maltose functionalized silver clusters will bind to any protein. However, it was observed that the characteristic property (*i.e.* fluorescence and colloidal stability) of maltose functionalized AgC solution did not change on the addition of BSA (Fig. 5). Therefore, maltose functionalized AgC can only be used for the detection of specific glycoprotein Con-A.

The maltose functionalized red fluorescent AgC was used to label HeLa cells at different concentrations (Fig. 6 & S15†). It was seen that maltose functionalized red fluorescent silver cluster interact with HeLa cells. The MTT-based cell viability data showed that maltose functionalized red fluorescent silver clusters exhibit low toxicity in the labelling concentration (*i.e.* 270 μg mL^{-1}), as well as at higher concentrations (~500 μg mL^{-1}) (S13†). Small hydrodynamic size and the presence of maltose molecule on the surface of red fluorescent AgC helps to label the HeLa cells. The fluorescence property of AgC allowed the fluorescence based imaging of the labelled HeLa cell. Here, it was noticed from the zeta potential measurements that maltose functionalized AgC were negatively charged at a biological pH of 7.4. However, it still labelled the negatively charged cell membrane. This result showed that there may be some specific interactions between the glucose molecules of

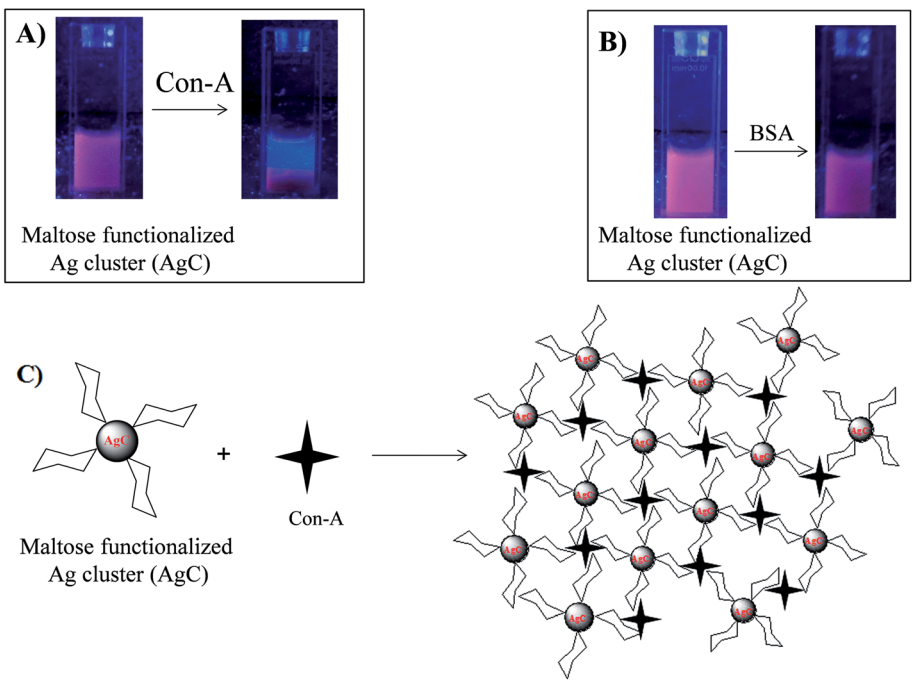

Fig. 5 Specific glycoprotein detection by maltose functionalized red fluorescent silver clusters (AgC). (A) Glycoprotein Con-A detection by maltose functionalized AgC. After the addition of Con-A, fluorescent AgC is precipitated from the solution (B) control experiment with BSA showing no AgC precipitation after the adding of BSA. (C) Schematic representation of Con-A detection by maltose functionalized AgC.

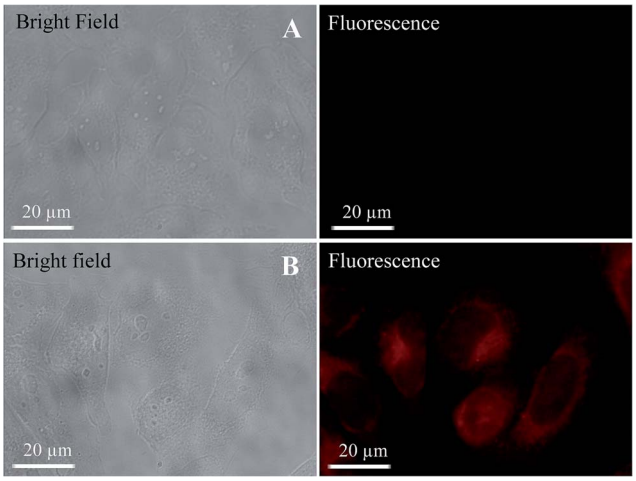

Fig. 6 (A) Upper panel shows the bright field and fluorescence image of HeLa cells without adding any red fluorescent AgC to the cell medium containing the HeLa cells. (B) The lower panel shows the labelling of HeLa cells by the maltose functionalized red fluorescent AgC with a concentration of 270 μg mL^{-1}.

maltose functionalized AgC and the cell membrane of the HeLa cells. Finally, red fluorescent AgC labelled HeLa were successfully imaged by conventional fluorescence microscopy.

Conclusion

Red fluorescent silver clusters (AgC) were synthesized by a simple one step method using cysteamine modified maltose molecule. The silver clusters showed a reasonably good fluoresce quantum yield with a good colloidal stability of hydrodynamic size <5 nm. This cluster also showed low toxicity to HeLa cells. Maltose functionalized red fluorescent AgC has been used for specific glycoprotein detection and cellular labeling applications. These maltose functionalized red fluorescent silver clusters can be used for sub cellular imaging and *in vivo* based applications.

Acknowledgements

S.B. acknowledges the financial support provided by University Grants Commission, Govt. of India through the Dr D. S. Kothari Post-Doctoral Fellowship and S.B. acknowledges Dr Nikhil Ranjan Jana for the support and encouragement during this work. S.B is thankful to Dr D. S. Kothari post-doctoral mentor Prof. S.K. Swain. A.C. acknowledges CSIR for providing the fellowship.

References

1 A. M. Derfus, W. C. W. Chen and S. N. Bhatia, *Nano Lett.*, 2004, **4**, 11–18.
2 C. Kirchner, T. Liedl, S. Kudera, T. Pellegrino, A. M. Javier, H. E. Gaub, S. Stolzle, N. Fertig and W. J. Parak, *Nano Lett.*, 2005, **5**, 331–338.
3 N. R. Jana, *Phys. Chem. Chem. Phys.*, 2011, **13**, 385–396.
4 L. M. Liz-Marzan, M. Giersig and P. Mulvaney, *Langmuir*, 1996, **12**, 4329–4335.
5 N. R. Jana, C. Earhart and J. Y. Ying, *Chem. Mater.*, 2007, **19**, 5074–5082.
6 S. Basiruddin, A. Saha, N. Pradhan and N. R. Jana, *J. Phys. Chem. C*, 2010, **114**, 11009–11017.
7 S. Basiruddin, A. Saha, R. Sarkar, M. Majumder and N. R. Jana, *Nanoscale*, 2010, **2**, 2561–2564.
8 N. R. Jana, P. K. Patra, A. Saha, S. Basiruddin and N. Pradhan, *J. Phys. Chem. C*, 2009, **113**, 21484–21492.
9 T. Pellegrino, L. Manna, S. Kudera, T. Liedl, D. Koktysh, A. L. Rogach, S. Keller, J. Radler, G. Natile and W. J. Parak, *Nano Lett.*, 2004, **4**, 703–707.
10 S. K. Bhunia and N. R. Jana, *ACS Appl. Mater. Interfaces*, 2011, **3**, 3335–3341.
11 P. Das, A. Saha, A. R. Maity, S. C. Ray and N. R. Jana, *Nanoscale*, 2013, **5**, 5732–5737.
12 S. K. Bhunia, A. Saha, A. R. Maity, S. C. Ray and N. R. Jana, *Sci. Rep.*, 2013, **3**, 1473.
13 A. R. Maity, S. Palmal, S. Basiruddin, N. S. Karan, S. Sarkar, N. Pradhan and N. R. Jana, *Nanoscale*, 2013, **5**, 5506–5513.
14 A. R. Maity, A. Chakraborty, A. Mondal and N. R. Jana, *Nanoscale*, 2014, **6**, 2752–2758.
15 N. Mohan, C. S. Chen, H. H. Hsieh, Y. C. Wu and H. C. Chang, *Nano Lett.*, 2010, **10**, 3692–3699.
16 X. L. Ren, Z. Z. Chen, X. W. Meng, D. Chen and F. Q. Tang, *Chem. Commun.*, 2012, **48**, 9504–9506.
17 S. H. Liu, F. Lu and J. J. Zhu, *Chem. Commun.*, 2011, **47**, 2661–2663.
18 L. Maretti, P. S. Billone, Y. Liu and J. C. Scaiano, *J. Am. Chem. Soc.*, 2009, **131**, 13972–13980.
19 T. Y. Zhou, M. C. Rong, Z. M. Cai, C. Y. J. Yang and X. Chen, *Nanoscale*, 2012, **4**, 4103–4106.
20 H. X. Xu and K. S. Suslick, *ACS Nano*, 2010, **4**, 3209–3214.
21 B. Adhikari and A. Banerjee, *Chem. Mater.*, 2010, **22**, 4364–4371.
22 S. Huang, C. Pfeiffer, J. Hollmann, S. Friede, J. J. C Chen, A. Beyer, B. Haas, K. Volz, W. Heimbrodt, J. M. M. Martos, W. Chang and W. J. Parak, *Langmuir*, 2012, **28**, 8915–8919.
23 U. Anand, S. Ghosh and S. Mukherjee, *J. Phys. Chem. Lett.*, 2012, **3**, 3605–3609.
24 J. J. Li, X. Q. Zhong, H. Q. Zhang, X. C. Le and J. J. Zhu, *Anal. Chem.*, 2012, **84**, 5170–5174.
25 A. K. Singh, R. Kanchanapally, Z. Fan, D. Senapati and P. C. Ray, *Chem. Commun.*, 2012, **48**, 9047–9049.
26 A. Mathew, P. R. Sajanlal and T. Pradeep, *J. Mater. Chem.*, 2011, **21**, 11205–11212.
27 S. Roy, A. Baral and A. Banerjee, *ACS Appl. Mater. Interfaces*, 2014, **6**, 4050–4056.
28 J. T. Petty, S. P. Story, J. C. Hsiang and R. M. Dickson, *J. Phys. Chem. Lett.*, 2013, **4**, 1148–1155.
29 Z. Z. Huang, F. Pu, Y. H. Lin, J. S. Ren and X. G. Qu, *Chem. Commun.*, 2011, **47**, 3487–3489.
30 W. W. Guo, J. P. Yuan, Q. Z. Dong and E. K. Wang, *J. Am. Chem. Soc.*, 2010, **132**, 932–934.
31 S. M. Choi, J. H. Yu, S. A. Patel, Y. L. Tzeng and R. M. Dickson, *Photochem. Photobiol. Sci.*, 2011, **10**, 109–115.

32 J. Sharma, H. C. Yeh, H. Yoo, J. H. Werner and J. S. Martinez, *Chem. Commun.*, 2011, **47**, 2294–2296.
33 Z. Shen, H. W. Duan and H. Frey, *Adv. Mater.*, 2007, **19**, 349–352.
34 T. Ohyanagi, N. Nagahori, K. Shimawaki, H. Hinou, T. Yamashita, A. Sasaki, T. Jin, T. Iwanaga, M. Kinjo and S. I. Nishimura, *J. Am. Chem. Soc.*, 2011, **133**, 12507–12517.
35 Y. N. Zhao, B. G. Trewyn, I. I. Slowing and V. S. Y. Lin, *J. Am. Chem. Soc.*, 2009, **131**, 8398.
36 K. S. Kim, W. Hur, S. J. Park, S. W. Hong, J. E. Choi, E. J. Goh, S. K. Yoon and S. K. Hahn, *ACS Nano*, 2010, **4**, 3005.
37 L. N. Cui, J. A. Cohen, K. E. Broaders, T. T. Beaudette and J. M. J. Frechet, *Bioconjugate Chem.*, 2011, **22**, 949.
38 M. Gary-Bobo, Y. Mir, C. Rouxel, D. Brevet, I. Basile, M. Maynadier, O. Vaillant, O. Mongin, M. Blanchard-Desce, A. Morere, M. Garcia, J. Durand and L. Raehm, *Angew. Chem., Int. Ed.*, 2011, **50**, 11425.
39 S. Basiruddin, A. R. Maity and N. R. Jana, *RSC Adv.*, 2012, **2**, 11915–11921.
40 F. M. Kelly and J. H. Johnston, *ACS Appl. Mater. Interfaces*, 2011, **3**, 1083–1092.